Hybrid multi-scale modeling of brain tumor progression

Francisco G. Vital-Lopez, Costas D. Maranas, Antonios Armaou

The Pennsylvania State University, Department of Chemical Engineering

Introduction

Glioblastoma multiforme are aggressive brain tumors that grow rapidly with remarkable invasive properties [1]. Median survival for patients receiving optimal treatment (which includes surgical resection, radiation, and chemotherapy) is only about 12 months, with a very small chance of long term survival [2]. The dismal prognosis for patients diagnosed with glioblastoma has sparked considerable efforts, clinically and otherwise, to understand the progression of this disease [3-9]. Mathematical models and computational tools are increasingly being accepted in cancer research as aids for visualizing and integrating information, testing different mechanism hypotheses and suggesting optimal treatment strategies [10-18].

The progression of a tumor is the ultimate outcome of several time and space dependent interacting processes which entail the combined intracellular and extracellular events that govern cell survival, proliferation, and migration, as well as angiogenic, inflammatory, and immune responses. Modeling and computations have already made significant headway by introducing quantitative abstractions of key signaling cascades (e.g., EGFR, VEGFR) that direct the cell's response to extracellular stimuli at the micro-scale [19-21] as well as tumor evolution descriptions [18, 22-25] at the macro-scale. Brain tumor models are a subset of a broad spectrum of general tumor progression models that vary in their level of detail [26-30].

Mathematically, one of the most sophisticated frameworks is the so called agent-based modeling. The key idea of this approach is to capture the evolution of a tumor as the result of the collective behavior of individual cells. In turn, the behavior of every cell is predicted by a set of rules parameterized by the level of key biochemical cues [18, 23]. However, mathematical and computational requirements have driven these initial attempts to use simplified descriptions of the temporal-spatial distribution of extracellular species, the intracellular events or both. In this work, we present a multi-scale agent-based model of describes the progression of a brain tumor (i.e., glioblastoma multiforme) by capturing in detail the interplay between the temporal-spatial distribution of key biochemical and the intracellular signaling pathways that determine the fate of every tumor cell. In the following sections we present a brief description of the model and the main simulation results.

Model description

We developed a multiscale/multiresolution integration of dynamic extracellular and intracellular environments to describe the progression of a brain tumor. The main focus of this work is to establish a model's framework to describe tumor growth and invasion resulting from the proliferation and migration of individual tumor cells under biologically relevant conditions that consider both internal cell dynamics and the surrounding extracellular matrix. To achieve this goal, a large number of biochemical components of both the intra- and extra-cellular domains were integrated to capture the principal characteristics of tumor progression. Specifically, we consider that the state of every tumor cell (i.e., proliferating, migrating, quiescent or necrotic) will be determined by the level of activation of the Ras-Raf-MEK-ERK cascade and the local glucose and oxygen levels. The Ras-Raf-MEK-ERK cascade is triggered by the activation of the EGF receptor (EGFR) by the transforming growth factor α (TGFα) which diffuses from the blood vessels and also is produced by the necrotic tumor cells. The computational details of the various different components of the model are discussed below.

We consider a 2D extracellular environment, glucose, oxygen and TGFα concentrations are assumed to be continuous fields (thus described by a set of PDEs) and the cells are treated as discrete entities that may occupy a lattice point on a regular square grid. Healthy cells are assumed to consume glucose and oxygen at a constant rate

and are destroyed on contact by invading tumor cells. The parameters of extracellular model were collected from the open literature [18, 22, 38, 39] when available or estimated to fit the reported average glucose, oxygen and TGFα concentrations in the brain [40, 41]. Tumor cells also were assumed to modify the extracellular matrix, resulting in a decrease of the effective diffusion coefficients [42]. Blood vessel provided the necessary nutrients to the tumor cells, i.e., glucose, oxygen and TGFα. When encircled by proliferating tumor cells, vessels in the brain can become compressed and destabilized (vessel co-option) [43]. For simplicity reasons, it was assumed in our model that the tumor compresses a vessel when tumor cell proliferates into the space corresponding to the vessel. The vessel is then completely degraded and the tumor occupies the vessel space in its entirety. As stated above, tumor cells can be necrotic, quiescent, proliferating or migrating depending on the local concentration of glucose and oxygen and the activation level of their MAPK pathway. Viable tumor cells (i.e. non-necrotic cells) consume glucose and oxygen at higher rates than normal cells and produce TGFα at rate determined by intracellular signaling. Necrotic cells were assumed to be completely inert, simply occupying space. The intracellular MAPK pathway is represented by a set of ODEs [19] to calculate the TGFα dependent activation level of ERK and the amount of autocrine TGFα produced.

Mathematically, the tumor growth process is mathematically represented by the following hybrid system of partial and ordinary differential equations,

$$\begin{aligned} &\partial_t C_{extra} = \nabla \cdot (D(z)\nabla C_{extra}) + S(z, C_{extra}, C_{intra,i}) - R(z, C_{extra}, C_{intra,i}), \quad C_{extra} \in \Omega \\ &\partial_z C_{extra} = Q(C_{extra}), \quad C_{extra} \in \Gamma \\ &d_t C_{intra,i} = f_i(C_{extra}, C_{intra,i}), \quad i = 1,\ldots,N \end{aligned} \tag{1}$$

where C_{extra} denotes the concentrations of extracellular species (i.e., the nutrients, growth factors, etc.), C_{intra} denotes the concentration of the intracellular species and N their number (N = 14 in the current model). Ω is defined as the computational domain of the PDEs and Γ is the boundary of Ω. $Q(\cdot)$ specifies the Neumann boundary condition. $S(\cdot)$ and $R(\cdot)$ refer to production and consumption terms respectively. $D(z)$ is the diffusion coefficient which depends on the location of the tumor cells and f_i are the right-hand side functions of the ODEs describing the intracellular dynamics.

The simulation is started with the system at steady-state with the tissue consisting of only normal cells, at which time, a small core of 16 cancer cells (a 4×4 square) is introduced at the center of the domain. At every time step (Δt), the extracellular (PDEs) model is integrated to determine the glucose, oxygen and TGFα concentration profiles (see Fig. 1). These concentrations are inputs to the intracellular model for every cell, which is integrated to determine the ERK activation and the TGFα production rate, which then becomes an input to the PDE, which

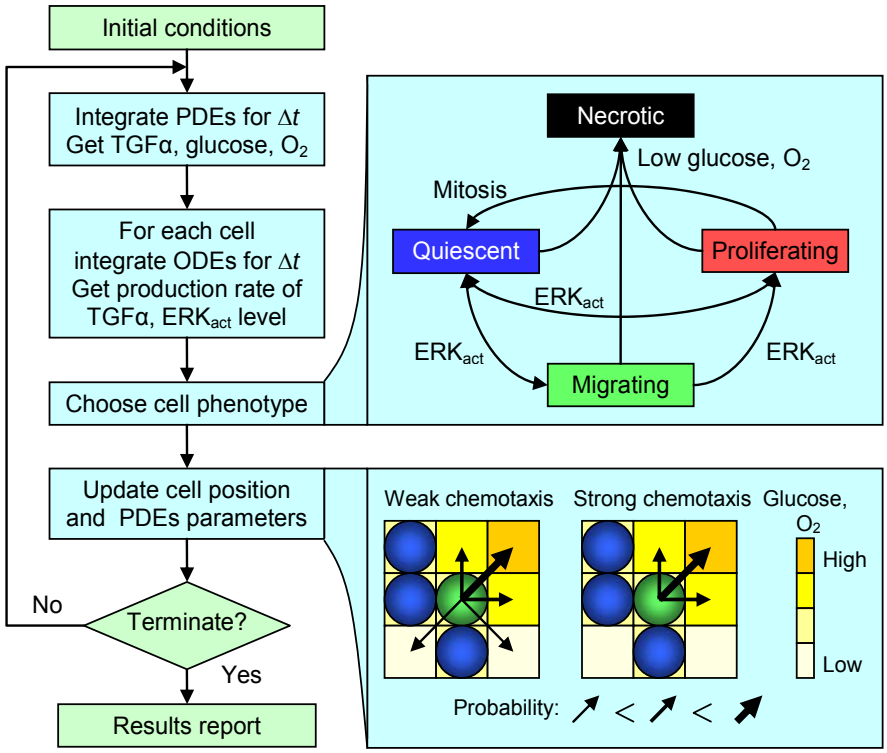

Figure 1. Simulation scheme of the multiscale tumor growth model. The tags close to the arrows (top-right box) indicate the governing variables for the transitions between phenotypes. Single and double head arrows indicate irreversible and reversible transitions, respectively. The simulation is terminated when a tumor cell reaches the border of the regular grid or the simulation time has been reached.

is integrated again until both the intracellular and extracellular models report the same value for TGFα. The phenotype of every cell is then determined depending on the level of glucose, oxygen and ERK activation and the position of cells and spatial dependent parameters are updated. The integration proceeds then in time until a cancerous cell reaches the boundary of the simulation domain or a pre-specified time limit is reached. The evolution rules to determine the phenotype of each cell are as follows:

- The probability of a viable tumor cell to remain alive depends on the local glucose and oxygen concentrations; there is a high probability it will become necrotic if their levels drop below a pre-specified threshold.
- If a viable cell "survives", then its phenotype is decided by a biased random process depending on the strength of the ERK activation. The decision process assigns to the cell a higher probability to become (or remain) quiescent, migrate or proliferate for low, medium or high ERK levels, respectively; the phenomenological threshold values are based on experimental observations [44].
- A cell that proliferates grows at a rate that depends on the glucose and oxygen concentrations; it will eventually divide if there is a free space in its neighborhood (i.e., not occupied by another cancer cell), otherwise it will become quiescent.
- Similarly, a tumor cell with migrating phenotype can move only to a free space on its neighborhood. In order to select the direction where the cell will move, we are considering two mechanisms: the first one, called weak chemotaxis, is similar to the biased random walk of [45] where the cell can move to any free space in its neighborhood with a probability parameterized by the glucose and oxygen levels. In the second one, called strong chemotaxis, is again a biased random walk were the cell movement is only allowed to free spaces where the glucose and oxygen concentrations are at least as high as in its current location.

The motivation for exploring the effect of these mechanisms is the observation that trajectories of migrating glioblastoma cell lines *in vitro* range from practically random to very close to linear [46]. This difference in the migration mechanism results in significantly different tumor morphology as will be shown in the following section.

Simulation results

Several simulations were performed to assess the growth patterns generated by the model under various extracellular conditions. In our initial simulation, the domain included regularly-spaced blood vessels to allow the sensitivity analysis of the basic system parameters. We subsequently simulated the tumor evolution in a larger domain with an irregular blood vessel distribution (Fig. 2) and evaluated the effect of strong vs. weak chemotaxis. Herein we present the simulation results for the latest case, focusing primarily on the tumor size and shape.

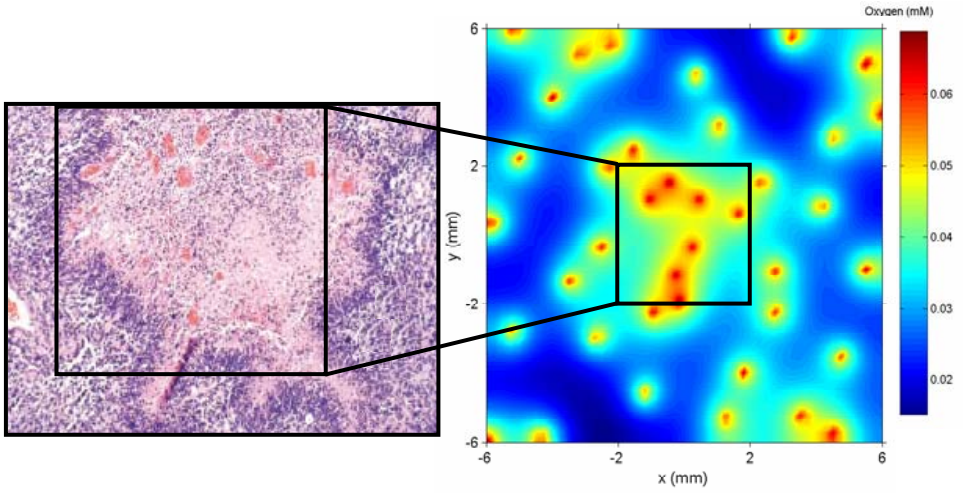

Figure 5. Spatial domain with irregular distribution of blood vessels. The graph at the right shows the initial oxygen concentration where the red spots correspond to the location of blood vessels. Tumor progression takes place in the central square whereas the surrounding is a buffer region. The vessels in the central square try to mimic the distribution of the vessels in the glioblastoma shown in the left picture.

Fig. 3a shows a large domain simulation with an irregular distribution of blood vessels under weak chemotaxis conditions. It is

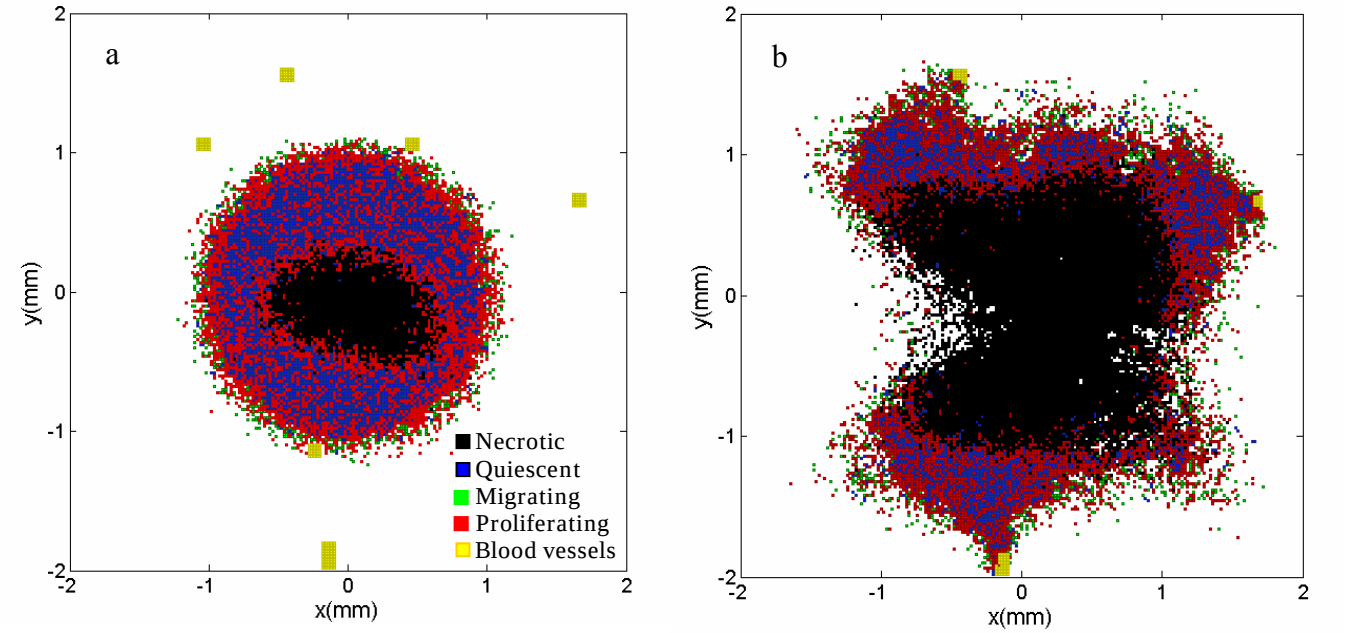

Figure 3. Snapshots of the brain tumor growing on a irregularly-spaced blood vessels at day 40. Cell migration directed by weak chemotaxis (a) and by strong chemotaxis (b).

apparent that weak chemotaxis conditions lead to tumors with regular, compact, circular shapes irrespective of the distribution of blood vessels. The effects of the irregular domain can be seen in the varying thickness of the shell of viable cells, and in the irregular shape of the necrotic core. We point out that at the end of the simulation, four vessels have been degenerated.

The results for the large domain simulation with irregularly distributed blood vessels and strong chemotaxis are shown in Fig. 3b. The majority of the tumor cells initially migrate to surround the closest blood vessel at day 10 (No shown). The tumor core started growing at this location, destroying the vessel by day 14. Once the source of nutrients was eliminated, the cells immediately began to migrate away from this point towards other vessels. It appears that upon reaching a vessel, the migrating cells remain close to it until the vessel is destroyed, and then resume their search for a new vessel. In contrast to the weak chemotaxis simulations, the topology of the vessels network has a significant role on the shape of the tumor. When a blood vessel is destroyed, tumor cells surrounding that vessel must escape and migrate to another vessel to avoid becoming necrotic. This may create a discontinuous shell of viable cells, which can put necrotic tumor cells in direct contact with (probably also necrotic) normal cells. A fundamental insight achieved by comparing the simulations shown in Fig. 3a and b is that chemotaxis conditions dominate the invasive nature of a tumor, and that strong chemotaxis results in an aggressive and invasive tumor type, possibly similar to that of glioblastomas (compare with Fig 2). The model predicts a substantially higher growth rate of the tumor driven under strong chemotaxis conditions. It is evident that the effects of strong vs. weak chemotaxis are numerous and significant, and the evident differences between the two simulations are thought provoking. Whereas the compact tumor driven by weak chemotaxis reached only three vessels by day 40, the strong chemotaxis driven tumor reached all vessels within the domain by day 40. Lower TGFα levels were found in more invasive tumor, but since they were higher than the threshold needed to activate ERK, the lower levels did not decrease cell migration. While at day 40 the number of viable cells in both simulations was similar (the weak chemotaxis tumor had 7,642 viable cells and the strong chemotaxis tumor had 8,138 viable cells), the number of necrotic cells was significantly greater in the strong chemotaxis tumor (8069 vs. 1717) that in the weak chemotaxis tumor. The irregular shaped tumor has a much larger tumor/normal tissue interface compared to a circular shaped tumor. The significance of these differences raises the need for further investigation.

Conclusions

The development of therapeutics for solid cancers requires a better understanding of tumor growth and progression. Tumor progression depends on the intricate interplay between biological processes that span multiple length scales from the molecular to the macroscopic. Mathematical modeling and computations can be efficiently used to organize and integrate the ever increasing experimental data as well as powerful tools to explore and generate new testable hypothesis. In this work we presented a multi-scale agent-based model to simulate the progression of a brain tumor. We used the model to explore hypothesis regarding the mechanisms by which tumor cell migrate. Simulations results suggest that ability of the migrating cells to sense the gradients of important biochemical cues such as nutrients and growth factors can be determinant in the invasive properties of the tumor. Furthermore, the model was able to produce *in silico* tumors with similar morphology to that of actual brain tumors. This model will be the starting point to construct a more complete model that includes more and more detailed descriptions signaling pathways (e.g., PI3K-Akt, PLCγ), tumor induced angiogenesis, pharmacokinetics/pharmacodynamics and its extension to a 3D space.

References

1. Louis, D.N., *Molecular pathology of malignant gliomas.* Annu Rev Pathol, 2006. **1**: p. 97-117.
2. Scott, J.N., et al., *Long-term glioblastoma multiforme survivors: a population-based study.* Canadian Journal of Neurological Sciences, 1998. **25**(3): p. 197-201.
3. Giese, A., et al., *Cost of migration: Invasion of malignant gliomas and implications for treatment.* Journal of Clinical Oncology, 2003. **21**(8): p. 1624-1636.
4. Stupp, R., et al., *Changing paradigms - An update on the multidisciplinary management of malignant glioma.* Oncologist, 2006. **11**(2): p. 165-180.
5. Maher, E.A., et al., *Malignant glioma: genetics and biology of a grave matter.* Genes & Development, 2001. **15**(11): p. 1311-1333.
6. Rao, J.S., *Molecular mechanisms of glioma invasiveness: The role of proteases.* Nature Reviews Cancer, 2003. **3**(7): p. 489-501.
7. Hamstra, D.A., et al., *Evaluation of the functional diffusion map as an early biomarker of time-to-progression and overall survival in high-grade glioma.* Proceedings of the National Academy of Sciences of the United States of America, 2005. **102**(46): p. 16759-16764.
8. Friedman, H.S., T. Kerby, and H. Calvert, *Temozolomide and treatment of malignant glioma.* Clinical Cancer Research, 2000. **6**(7): p. 2585-2597.
9. Dent, P., et al., *MAPK pathways in radiation responses.* Oncogene, 2003. **22**(37): p. 5885-5896.
10. Aubert, M., et al., *A cellular automaton model for the migration of glioma cells.* Physical Biology, 2006. **3**(2): p. 93-100.
11. Jbabdi, S., et al., *Simulation of anisotropic growth of low-grade gliomas using diffusion tensor imaging.* Magnetic Resonance in Medicine, 2005. **54**(3): p. 616-624.
12. MacArthur, B.D., C.P. Please, and G.J. Pettet, *A mathematical model of dynamic glioma-host interactions: receptor-mediated invasion and local proteolysis.* Mathematical Medicine and Biology-a Journal of the Ima, 2005. **22**(3): p. 247-264.
13. Zheng, X., S.M. Wise, and V. Cristini, *Nonlinear simulation of tumor necrosis, neo-vascularization and tissue invasion via an adaptive finite-element/level-set method.* Bulletin of Mathematical Biology, 2005. **67**(2): p. 211-259.
14. Frieboes, H.B., et al., *An integrated computational/experimental model of tumor invasion.* Cancer Research, 2006. **66**(3): p. 1597-1604.
15. Gevertz, J.L. and S. Torquato, *Modeling the effects of vasculature evolution on early brain tumor growth.* Journal of Theoretical Biology, 2006. **243**(4): p. 517-531.
16. Powathil, G., et al., *Mathematical modeling of brain tumors: effects of radiotherapy and chemotherapy.* Physics in Medicine and Biology, 2007. **52**(11): p. 3291-3306.
17. Stein, A.M., et al., *A mathematical model of glioblastoma tumor spheroid invasion in a three-dimensional in vitro experiment.* Biophysical Journal, 2007. **92**(1): p. 356-365.
18. Zhang, L., C.A. Athale, and T.S. Deisboeck, *Development of a three-dimensional multiscale agent-based tumor model: Simulating gene-protein interaction profiles, cell phenotypes and multicellular patterns in brain cancer.* Journal of Theoretical Biology, 2007. **244**(1): p. 96-107.
19. Maly, I.V., H.S. Wiley, and D.A. Lauffenburger, *Self-organization of polarized cell signaling via autocrine circuits: Computational model analysis.* Biophysical Journal, 2004. **86**(1): p. 10-22.

20. Mac Gabhann, F., M.T. Yang, and A.S. Popel, *Monte Carlo simulations of VEGF binding to cell surface receptors in vitro.* Biochimica Et Biophysica Acta-Molecular Cell Research, 2005. **1746**(2): p. 95-107.
21. Hornberg, J.J., et al., *Control of MAPK signalling: from complexity to what really matters.* Oncogene, 2005. **24**(36): p. 5533-5542.
22. Jiang, Y., et al., *A multiscale model for avascular tumor growth.* Biophysical Journal, 2005. **89**(6): p. 3884-3894.
23. Betteridge, R., et al., *The impact of cell crowding and active cell movement on vascular tumour growth.* Networks and Heterogeneous Media, 2006. **1**(4): p. 515-535.
24. Anderson, A.R.A., et al., *Tumor morphology and phenotypic evolution driven by selective pressure from the microenvironment.* Cell, 2006. **127**(5): p. 905-915.
25. Dyson, J., et al., *An age and spatially structured model of tumor invasion with haptotaxis.* Discrete and Continuous Dynamical Systems-Series B, 2007. **8**(1): p. 45-60.
26. Arakelyan, L., Y. Merbl, and Z. Agur, *Vessel maturation effects on tumour growth: validation of a computer model in implanted human ovarian carcinoma spheroids.* European Journal of Cancer, 2005. **41**(1): p. 159-167.
27. Byrne, H.M., et al., *Modelling the response of vascular tumours to chemotherapy: A multiscale approach.* Mathematical Models & Methods in Applied Sciences, 2006. **16**(7): p. 1219-1241.
28. Kohandel, M., et al., *Dynamics of tumor growth and combination of anti-angiogenic and cytotoxic therapies.* Phys Med Biol, 2007. **52**(13): p. 3665-77.
29. Li, X.R., et al., *Nonlinear three-dimensional simulation of solid tumor growth.* Discrete and Continuous Dynamical Systems-Series B, 2007. **7**(3): p. 581-604.
30. Macklin, P. and J. Lowengrub, *Nonlinear simulation of the effect of microenvironment on tumor growth.* Journal of Theoretical Biology, 2007. **245**(4): p. 677-704.
31. Behin, A., et al., *Primary brain tumours in adults.* Lancet, 2003. **361**(9354): p. 323-331.
32. Arwert, E., et al., *Visualizing the dynamics of EGFR activity and antiglioma therapies in vivo.* Cancer Research, 2007. **67**(15): p. 7335-7342.
33. Krueger, J.S., et al., *Temporal and quantitative regulation of mitogen-activated protein kinase (MAPK) modulates cell motility and invasion.* Oncogene, 2001. **20**(31): p. 4209-4218.
34. Sharif, A., et al., *Transforming growth factor alpha acts as a gliatrophin for mouse and human astrocytes.* Oncogene, 2006. **25**(29): p. 4076-4085.
35. Teo, C.S., et al., *Transient interstitial fluid flow in brain tumors: Effect on drug delivery.* Chemical Engineering Science, 2005. **60**(17): p. 4803-4821.
36. Jain, R.K., *Delivery of molecular and cellular medicine to solid tumors.* Advanced Drug Delivery Reviews, 2001. **46**(1-3): p. 149-168.
37. Harashima, H., et al., *Pharmacokinetic/pharmacodynamic modeling of antitumor agents encapsulated into liposomes.* Advanced Drug Delivery Reviews, 1999. **40**(1-2): p. 39-61.
38. Hudetz, A.G., *Mathematical model of oxygen transport in the cerebral cortex.* Brain Research, 1999. **817**(1-2): p. 75-83.
39. Dienel, G.A. and L. Hertz, *Glucose and lactate metabolism during brain activation.* Journal of Neuroscience Research, 2001. **66**(5): p. 824-838.
40. Evans, S.M. and C.J. Koch, *Prognostic significance of tumor oxygenation in humans.* Cancer Letters, 2003. **195**(1): p. 1-16.
41. Erecinska, M. and I.A. Silver, *Tissue oxygen tension and brain sensitivity to hypoxia.* Respiration Physiology, 2001. **128**(3): p. 263-276.
42. Zamecnik, J., *The extracellular space and matrix of gliomas.* Acta Neuropathologica, 2005. **110**(5): p. 435-442.
43. Jain, R.K., et al., *Angiogenesis in brain tumours.* Nature Reviews Neuroscience, 2007. **8**(8): p. 610-622.
44. Giese, A., et al., *Dichotomy of astrocytoma migration and proliferation.* International Journal of Cancer, 1996. **67**(2): p. 275-282.
45. Anderson, A.R.A. and M.A.J. Chaplain, *Continuous and discrete mathematical models of tumor-induced angiogenesis.* Bulletin of Mathematical Biology, 1998. **60**(5): p. 857-899.
46. Demuth, T., et al., *Migratory activity of human glioma cell lines in vitro assessed by continuous single cell observation.* Clinical & Experimental Metastasis, 2001. **18**(7): p. 589-597.